# Robust feedback lateral control using a parameterized LFR model and DGK-iteration

*A. Schirrer*⋆*, C. Westermayer*⋆*, M. Hemedi*⋆*, and M. Kozek*⋆
⋆*Institute of Mechanics and Mechatronics*
Vienna University of Technology
*Wiedner Hauptstr. 8, 1040 Vienna, Austria*

## Abstract

This paper shows results, performance and limitations of robust lateral control law designs for a large, flexible blended wing body passenger aircraft. The aircraft dynamics is pre-shaped by a robust inner loop control law aiming at stabilization, basic response shaping, and flexible mode damping. The presented designs aim to further improve vibration damping of the main flexible modes despite significant parameter-dependent plant variations. The resulting high-dimensional robust control design problem is addressed via the DGK-iteration method applied to a parameterized reduced-order integrated model of both rigid-body and flexible dynamics in Linear Fractional Representation (LFR). While a high-accuracy LFR yields a prohibitive problem size for today's design tools, simplified uncertainty parameterizations result in a successful control design. Different modeling approaches are compared and discussed with respect to the trade-off between achievable control performance, robustness, and problem size/controller order.

## 1. Introduction

Flexible aircraft control is by now a widely studied task (see for example [8], [10], [11], [23], or [24]), driven by potential weight savings and thus potentially increased fuel efficiency. One particularly interesting concept in civil aviation are blended wing body (BWB) configurations which bear an additional potential of reduced fuel consumption per passenger, but they also pose new challenges in multi-objective control design [13]: potential (cross-)coupling of longitudinal and lateral motion (and low-frequency flexible modes), possible open-loop instability, as well as a high performance demands in loads alleviation, vibration reduction, and maneuver shaping.

Flight and structural control laws are commonly built using robust control design methods to ensure satisfactory control performance also in the presence of plant uncertainties. The DK-iteration and more recently the DGK-iteration or mixed-$\mu$-synthesis are well-known design tools to generate such control laws [2], [20], [25].

This paper presents a state-of-the-art flight control design for a novel application: control of the lateral dynamics of a large, flexible BWB passenger aircraft. A multitude of stringent constraints and goals are given in the time and frequency domain. An initial controller is designed using robust modal control design [12], [18] to achieve some of the goals most closely related to eigenstructure assignment. Based on the pre-shaped plant, a parameterized high-accuracy parameterized Linear Fractional Representation (LFR) is built which serves as basis for robust feedback control design by DGK-iteration. Due to high-dimensional parameter dependency and loose bounds in current $\mu$ analysis tools, this synthesis task faces computational difficulties given today's workstation computing performance and numeric properties of the algorithms. Thus, ways to reduce design complexity and improve resulting robust control performance are tested and assessed in terms of performance, robustness, tractability, and problem size. A high-accuracy parametric LFR as well as various simplified LFR formulations are utilized in subsequent design attempts.

A general integrated methodology for multi-objective robust control design has been presented in [15]. Previous, closely related studies started on a larger BWB passenger aircraft pre-design model: for LQ-based lateral control designs see [16], the application of a genetic algorithm for parameter optimization of a multiobjective $\mathcal{H}_\infty$ DK-iteration design has been treated in [19]. Using a Youla parameterization of the feedback control loop, a convex controller synthesis for lateral BWB control has been performed in [18] with a subsequent scheduled feedforward control design in [17]. Longitudinal BWB control using LPV control concepts has been studied in [22]. The models of the currently

studied BWB passenger aircraft are obtained by highly detailed modeling and are expected to yield more reliable results for control validation.

This paper is structured as follows: Sec. 2 introduces the aircraft model, provides an overview on its open-loop characteristics, and formulates the envisaged control goals. Sec. 3 outlines the control design variants and attempts that were carried out to fulfill the control goals. In Sec. 4, the final design is validated at all validation cases of the aircraft model and its performance is assessed. The main issues from a design perspective are discussed. Sec. 5 concludes the paper.

## 2. System model

Longitudinal and lateral flight mechanics and aeroelastic effects of a large blended wing body passenger aircraft predesign and their coupling were modeled in an integrated fashion by the authors' project partners [21]. These models consider a redesigned, downsized BWB configuration as compared to earlier studies (see [16], [19], [18], and [17]).

This study only considers the lateral dynamics as well as the flexible structure modes and aerodynamic lag states to design and validate the lateral control laws. A set of $k = 30$ linearized state space systems $\boldsymbol{P}_i$, $i = 1, \ldots, k$ for various parameter values of fuel filling level and CG position (at fixed cruise altitude and airspeed) is available:

$$\dot{\boldsymbol{x}} = \boldsymbol{A}_i \boldsymbol{x} + \boldsymbol{B}_i \boldsymbol{u} \tag{1}$$

$$\boldsymbol{y} = \boldsymbol{C}_i \boldsymbol{x} + \boldsymbol{D}_i \boldsymbol{u}. \tag{2}$$

The state vector $\boldsymbol{x}$ is composed of 4 flight-mechanic states (side slip angle $\beta$, roll rate $p$, yaw rate $r$, roll angle $\phi$), 12 elastic states (6 structural antisymmetric modes), as well as 7 aerodynamic lag states. The integrator states $\psi$ (yaw angle) and $y$ (horizontal displacement) are neglected in this study. These systems are augmented by actuator and sensor dynamics.

Utilized inputs $\boldsymbol{u}$ for control design are:

- Symmetric rudder deflection and rate $u_{\mathrm{RU}}, \dot{u}_{\mathrm{RU}}$
- Combined antisymmetric aileron deflection and rate: middle and inner ailerons are deflected equally ($u_{\mathrm{AIL}}, \dot{u}_{\mathrm{AIL}}$)
- Antisymmetric outer aileron deflection and rate ($u_{\mathrm{OA}}, \dot{u}_{\mathrm{OA}}$)

The actuator dynamics $\boldsymbol{G}_{\mathrm{act}}$ are modeled via 2$^{\mathrm{nd}}$-order low-pass filters as a low-order approximation of physically modeled control surfaces and actuation system dynamics. These dynamics model both the actual surface deflection as well as its rate $\left([u_j, \dot{u}_j]^T = \boldsymbol{G}_{\mathrm{act},j}\, u_{\mathrm{command},j}\right)$.

Utilized outputs $\boldsymbol{y}$ for control design are:

1. Side slip angle $\beta$
2. Roll angle $\phi$
3. Roll rate $p$
4. Yaw rate $r$
5. Antisymmetric modal acceleration sensor $Nz_{\mathrm{lat.law}} = Nz_{\mathrm{r.wingtip}} - Nz_{\mathrm{l.wingtip}}$ where $Nz_{\mathrm{r.wingtip}}$ and $Nz_{\mathrm{l.wingtip}}$ are vertical accelerations at the right and left wingtips, respectively,

which are each considered subject to time delays due to signal processing latencies (160 ms for outputs (1-4), 60 ms for output (5)), modeled via 2$^{\mathrm{nd}}$-order Padé approximations. Additionally 2$^{\mathrm{nd}}$-order low-pass Butterworth filters are applied to outputs (1-4). The sensor dynamics is collected into $\boldsymbol{G}_{\mathrm{sens}}$, and the augmented system $\widetilde{\boldsymbol{P}}_i = \boldsymbol{G}_{\mathrm{sens}} \boldsymbol{P}_i \boldsymbol{G}_{\mathrm{act}}$ is of order 47.

Additional exogenous input and output signals for validation are considered - a wind gust disturbance input (lateral wind speed $d = v_{\mathrm{lat}}$) as well as a structure load output $My_{\mathrm{wing}}$ (a cut moment at the wing).

### 2.1 Open-loop characteristics

The uncontrolled lateral aircraft dynamics shows a slowly unstable spiral mode for all considered mass cases at cruise flight conditions. Moreover, a prominent low-damped Dutch Roll (DR) mode between 0.7 and 0.9 $^{\text{rad}}/_{\text{s}}$ with a damping between 0.03 and 0.06 is present. Six relevant antisymmetric flexible modes are located between 10 and 50 $^{\text{rad}}/_{\text{s}}$ of which the first two (at approximately 10 and 20 $^{\text{rad}}/_{\text{s}}$, respectively) are considered critical for structure loads and comfort. Fig. 1 shows the gust $v_{\text{lat}}$ - wing load $My_{\text{wing}}$ response for the uncontrolled aircraft at all considered mass cases, as well as the response of the aircraft controlled by an initial robust pole placement controller which robustly stabilizes and assigns satisfactory rigid-body responses (see Sec. 3.1). However, as evident in Fig. 1, the low-frequency transfer magnitude from lateral gust to $My_{\text{wing}}$ is increased as a result of stabilization.

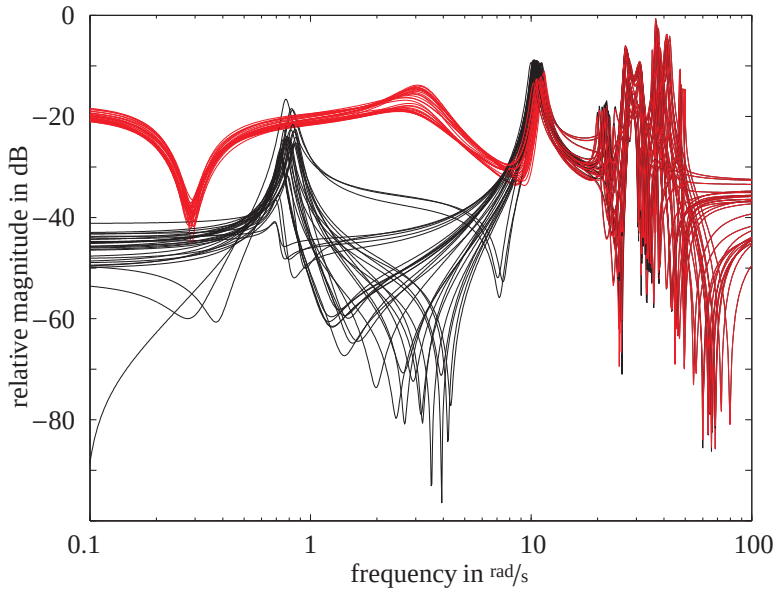


Figure 1: Bode magnitude plot of lateral wind $v_{\text{lat}}$ - wing cut moment $My_{\text{wing}}$ for all mass cases (black: open-loop, red: closed loop with initial stabilizing controller, see Sec. 3.1)

### 2.2 Control goals

The general control goals for lateral inner loop control are:

1. stabilize the aircraft
2. obtain high damping of the Dutch Roll mode
3. obtain sufficiently fast real / aperiodic remaining system dynamics to fulfill rise-time requirements on roll / side slip responses in 7 and 5 s, respectively
4. maximize damping of the first two flexible modes

These requirements all have to be fulfilled robustly for all admissible parameter cases in the viewed parameter space. They will all be addressed, as far as possible, by an initial control law which is designed through robust/insensitive eigenstructure assignment. However, further improvement of the vibration damping performance (goal 4) is possible when exploiting knowledge on the parameter dependency. Thus, the focus and main control goal of this work is to improve on goal 4.

## 3. Control design

### 3.1 Initial controller

In order to efficiently fulfill the requirements on the rigid-body response of the aircraft, a robust eigenstructure assignment approach is taken. Utilizing the Robust Modal Control Toolbox (see [12]), a low-order output feedback control law is generated which robustly assigns partial eigenstructure specifications (as in [18]). An output feedback controller $\boldsymbol{K}_{\text{init}}$ of dynamic order 1 is obtained. The initial controller is interconnected to the aircraft system models, forming a set of pre-shaped plants (each of dynamic order 48). Figure 1 shows the effect of this initial control law: the aircraft is robustly stabilized, hence it cannot be avoided that the static loads due to the disturbance are increased. The flight mechanic modes are assigned robustly to their desired locations and the responses are shaped as desired. Through eigenvector projection it is possible to reduce the first flexible mode robustly by about $-6$ dB. Fig. 1 shows the improved flexible mode damping and Fig. 2 shows the correctly and robustly shaped flight dynamic response characteristics. Note that it is not possible to directly and robustly increase flexible mode damping further with this design methodology.

### 3.2 Linear Fractional Representation of the parameterized, pre-shaped plants

By exploiting the structure of the parameter dependency of the plant, the damping of the first flexible modes is attempted to be further increased, without altering the other control goals (rigid-body response, stability). Therefore, an LFR description of this set of pre-shaped plants in the two parameters CG and fuel filling has been generated from the model grid (1)–(2) and validated by the authors' project partners analogous to the procedure in [9]. The aerodynamic lag states were removed for the LFR generation. A first, high-accuracy LFR has been generated which has 41 states and a $\boldsymbol{\Delta}$ block size of $40\times40$ (in which the two real-valued parameters are 9 and 31 times repeated, respectively). Later, due to computational difficulties with this level of complexity, a simplified parameterization has been generated which leads to a reduced-accuracy LFR with 33 states and a $13\times13$ $\boldsymbol{\Delta}$ block (8 and 5 times repeated, respectively).

Fig. 2 shows scaled, typical step responses (as modeled by the high-accuracy LFR) for several randomly sampled parameter values. The rigid-body response is considered satisfactorily shaped by the initial controller.

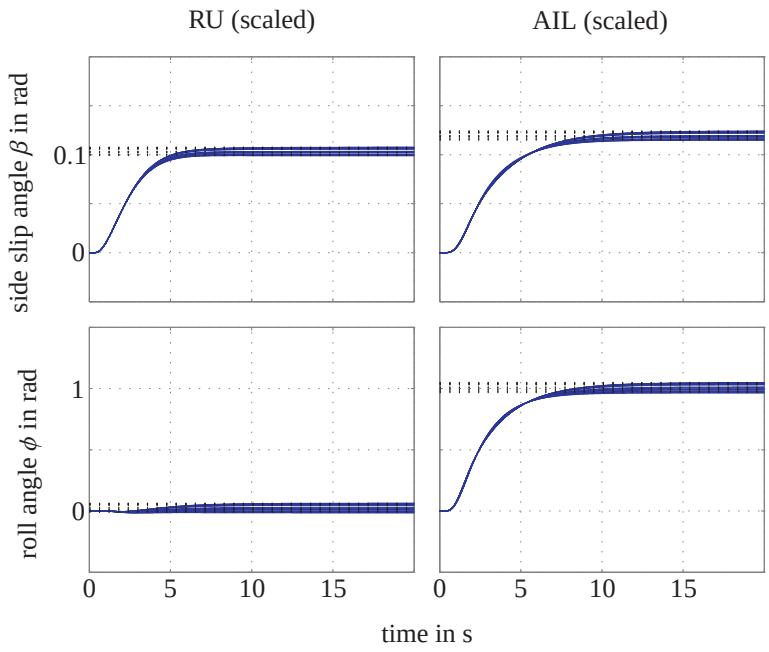


Figure 2: Step responses of the pre-shaped plants from rudder and ailerons to side slip and roll angles at random CG and fuel parameter values

### 3.3 DGK-iteration results

DGK-iteration is employed with the aim to generate a robust controller that fulfils the targeted control goals: to attenuate the first and second flexible modes, and thus reduce the gust-induced wing loads. For details on the involved robust control theory, fundamental definitions of linear fractional transforms/representation (LFTs/LFRs), the structured singular value ($\mu$), robust stability (RS), robust performance (RP), or the DK- and DGK-iteration algorithms the reader is referred to [2], [20], [25], and [7].

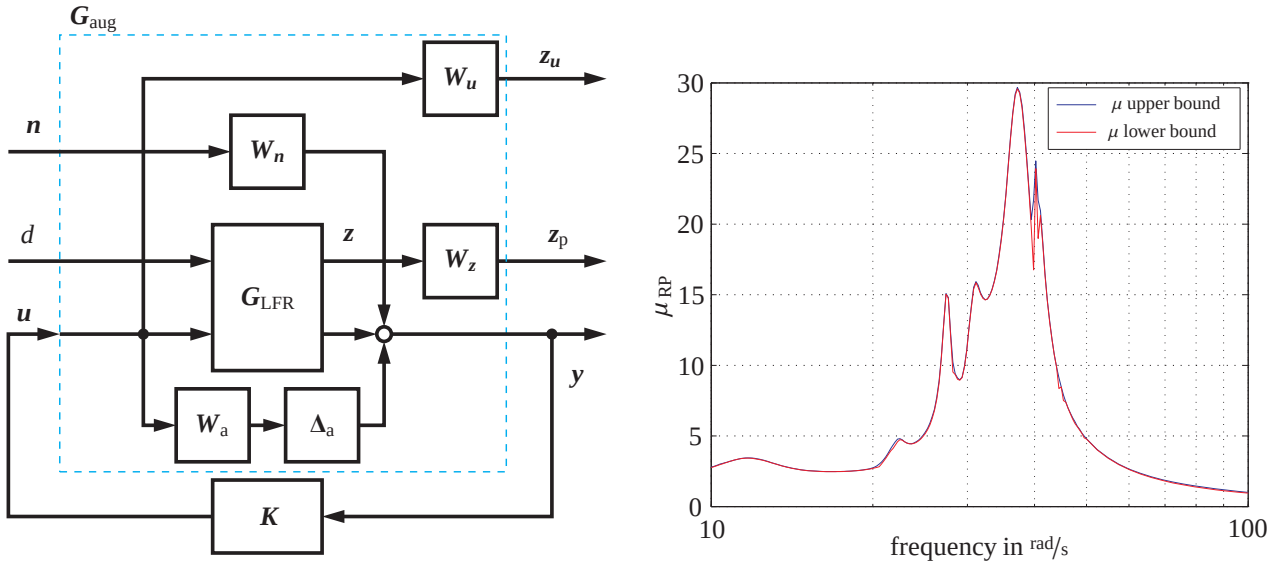


Figure 3: Design architecture for DGK-iteration (left), robust performance $\mu$ analysis results (right)

The control design architecture for control design via DGK-iteration is outlined in Fig. 3 (left). The system LFR $\boldsymbol{G}_{\text{LFR}}$ is augmented by the design weights $\boldsymbol{W}_{\text{a}}$, $\boldsymbol{W_n}$, $\boldsymbol{W_u}$, and $\boldsymbol{W_z}$ to obtain the augmented plant $\boldsymbol{G}_{\text{aug}}$, and $\boldsymbol{K}$ is the robust feedback LTI controller to be designed. The modeled signals are disturbance input $d = v_{\text{lat}}$, feedback control commands $\boldsymbol{u} = [u_{\text{RU,FB}}, u_{\text{AIL,FB}}, u_{\text{OA,FB}}]^T$, the performance outputs $\boldsymbol{z} = [My_{\text{wing}}, Nz_{\text{lat.law}}]^T$, the measured outputs $\boldsymbol{y} = [\beta, \phi, p, r, Nz_{\text{lat.law}}]^T$ with measurement noise $\boldsymbol{n}$, as well as the weighted output signals $\boldsymbol{z_u}$ and $\boldsymbol{z_p}$. The measurement noise weighted $\boldsymbol{W}_n$ and the additive uncertainty weight $\boldsymbol{W}_{\text{a}}$ serve as problem regularization terms and are chosen small and constant. The remaining weights are chosen to

- ensure well-scaled input/output magnitudes (via scaling inside $\boldsymbol{G}_{\text{LFR}}$),
- emphasize the 1st and 2nd wing bending modes in the performance path (via $\boldsymbol{W_z}$), and to
- limit the control input magnitudes to the admissible input range (via $\boldsymbol{W_u}$).

#### 3.3.1 DGK-design attempt with high-accuracy LFR

The results of a DGK-iteration run based on the high-accuracy LFR are shown in Fig. 3 (right). The robust performance $\mu$ value is much larger than 1 at all considered frequencies – it is clearly evident that the closed loop fails to achieve satisfactory control performance. In further studies it becomes evident that the bounds of the open loop robust stability $\mu$ value are very loose. This problem of convergence and the resulting conservativeness in the D- and G-scalings yield unsatisfactory results of the design. Note that only static scalings could be utilized in DGK-iteration design due to the problem size: The $\boldsymbol{\Delta}$-block contains $40 \times 40 = 1600$ entries. Fitting these with dynamic G- and D-scalings inflates the controller order quickly well above 1000 which is numerically and computationally infeasible.

One common heuristics to improve mixed-$\mu$ convergence is to add small, complex uncertainties to the existing real uncertainties. This was attempted first, however no improvement in $\mu$ bound convergence could be observed.

To overcome the encountered computational difficulties two simplification approaches will be taken and compared in the following.

### 3.3.2 DGK-design attempt with ad-hoc uncertainty model

Based on the observation that the perturbations of the flexible mode parameters are the main source of uncertainty, an ad-hoc uncertainty parameterization is attempted (see [23], [3], and [25] for similar attempts). The aircraft models are close to a modal form [6] in which a low-damped flexible mode is represented by a $2 \times 2$ submatrix of the system matrix $\boldsymbol{A}$:

$$\boldsymbol{A}_{\mathrm{m}i} = \begin{bmatrix} 0 & 1 \\ -\omega_i^2 & -2\zeta_i\omega_i \end{bmatrix}. \tag{3}$$

By replacing the $(2,1)$ and $(2,2)$ matrix elements with real-valued uncertain parameters which are confined to the intervals occurring across the model set, an efficient uncertainty representation with a small uncertainty matrix $\boldsymbol{\Delta}$ of size $2 \times 2$ per mode is obtained. Note that no other variations in the plant are considered, hence the uncertainty model is rather crude. The architecture shown in Fig. 3 is reused, but the plant LFR is replaced by its simplified version (with a $\boldsymbol{\Delta}$-block of $4 \times 4$). The achieved robust performance $\mu$ value is 2.7.

The obtained controller is of dynamic order 117 (due to dynamic D- and G-scalings) after few minutes of computation time on a standard office PC. This controller complexity is in general too high for implementation, so controller order reduction is needed subsequently.

Fig. 4 shows the performance singular values of the open- and closed-loop systems with the validation plants. It is evident that for most models the obtained controller performs well and achieves strong attenuation (about $-7$ dB) of the first and second flexible modes. However, in two (extremal) parameter cases the second flexible mode of the respective validation plant is destabilized. No simple means are available to ensure stability with these plants except for enlarging the uncertainty ranges which quickly destroys the obtained nominal performance.

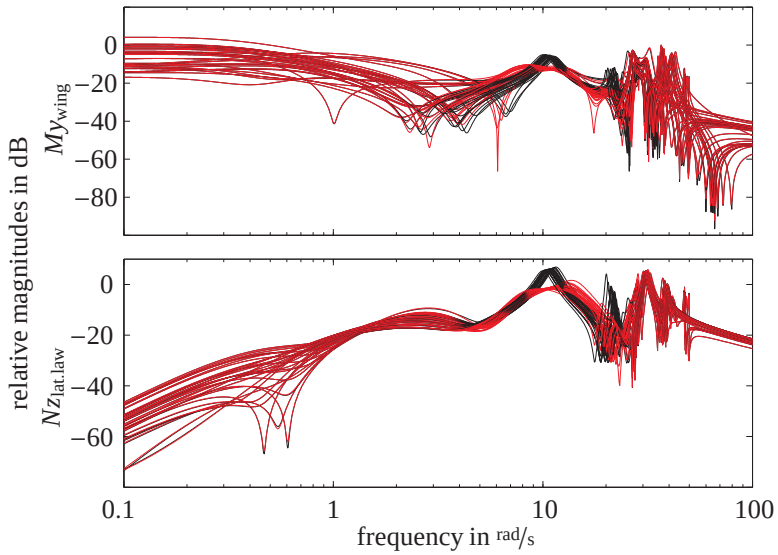


Figure 4: Bode magnitude plots of (von-Karman low-pass filtered) lateral wind $v_{\mathrm{lat}}$ - wing cut moment $My_{\mathrm{wing}}$ and modal acceleration signal $Nz_{\mathrm{lat.law}}$ for all mass cases (black: pre-shaped design plant, red: closed loop with robust controller, obtained by DGK-iteration on simplified design LFR)

### 3.3.3 DGK-design with reduced-accuracy LFR

In order to obtain a computationally manageable problem size, but still to obtain a robustly stabilizing and performing control law, a reduced-accuracy parameterized LFR has been generated. The weight shapes are chosen as depicted in Fig. 5 to emphasize the control effect on the first flexible mode. After several design iterations, it became clear that the large variation of the second flexible mode is a limiting factor in the design – therefore the weightings are adapted to avoid control action at the second flexible mode's frequency range.

Fig. 6 shows the unweighted and the weighted performance singular values of the unweighted (scaled) LFR and of the weighted design plant, randomly sampled in the uncertain set. The effect of the chosen weightings is clearly

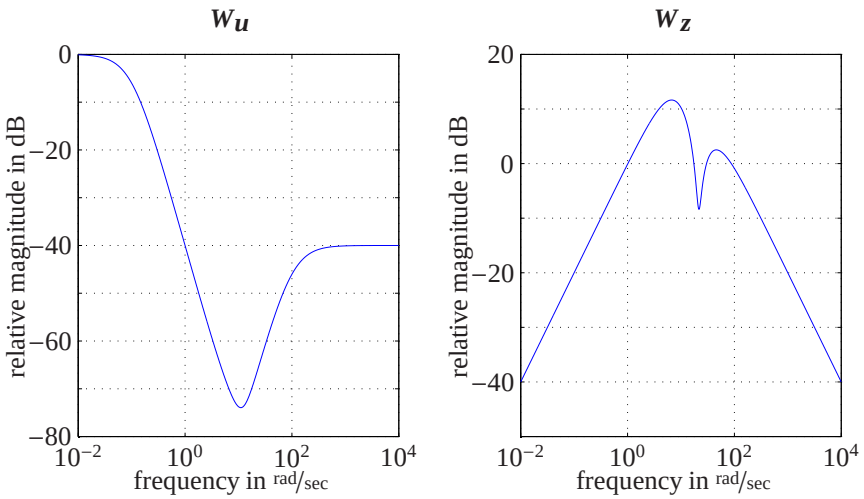


Figure 5: Weight shapes of $\boldsymbol{W}_u$ (left) and $\boldsymbol{W}_z$ (right): The control action is focused on the first wing bending mode (notch in $\boldsymbol{W}_u$, peak in $\boldsymbol{W}_z$). Additionally the 2nd flexible mode must be attenuated in the performance path to obtain robust performance.

visible – the strongly varying second mode is decreased in importance; the control design task focuses on the first flexible mode.

After the DGK-iteration run (20 iterations, $\boldsymbol{D}$- and $\boldsymbol{G}$-scalings up to order 4, grid of 284 frequencies, augmented design plant $\boldsymbol{P}_{\text{aug}}$ of order 59, 135 min computation time), a robust performance $\mu$ of 1.44 is obtained (as compared to an open-loop robust performance $\mu$ of 2.0), which is still larger than 1, but, as seen in Fig. 7, the robust stability $\mu$ value is less than 1. The figure shows also the nominal performance singular values (single weighted load performance outputs and all outputs combined) of the nominal closed loop $\boldsymbol{M}$ and thus shows the closed-loop system variation bounds as gap between the nominal singular values and the robust performance $\mu$ bound. The controller dynamic order is very high with 253 states. For implementation, (robust) controller order reduction must be performed, see [4] for a $\mu$-based approach. The high-order control law can be reduced by MATLAB's `reduce` command [2] with the option `'ErrorType','mult'` to order 30 virtually without performance loss. The underlying algorithm is a balanced stochastic model truncation (BST) via Schur's method [14].

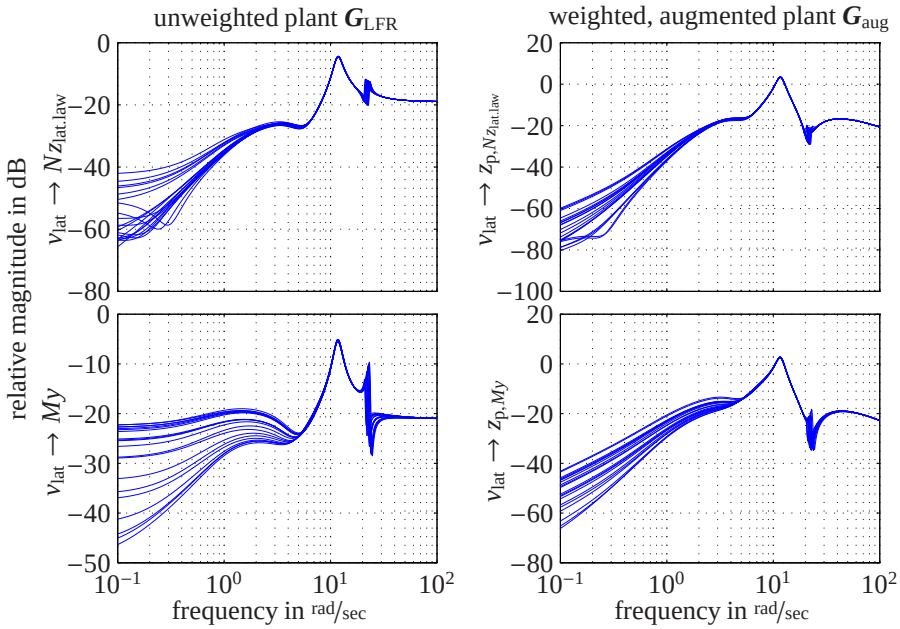


Figure 6: Scaled, unweighted (left) and weighted (right) magnitude plot of lateral gust - performance outputs as modeled by the reduced-complexity LFR, sampled at 20 random parameter points

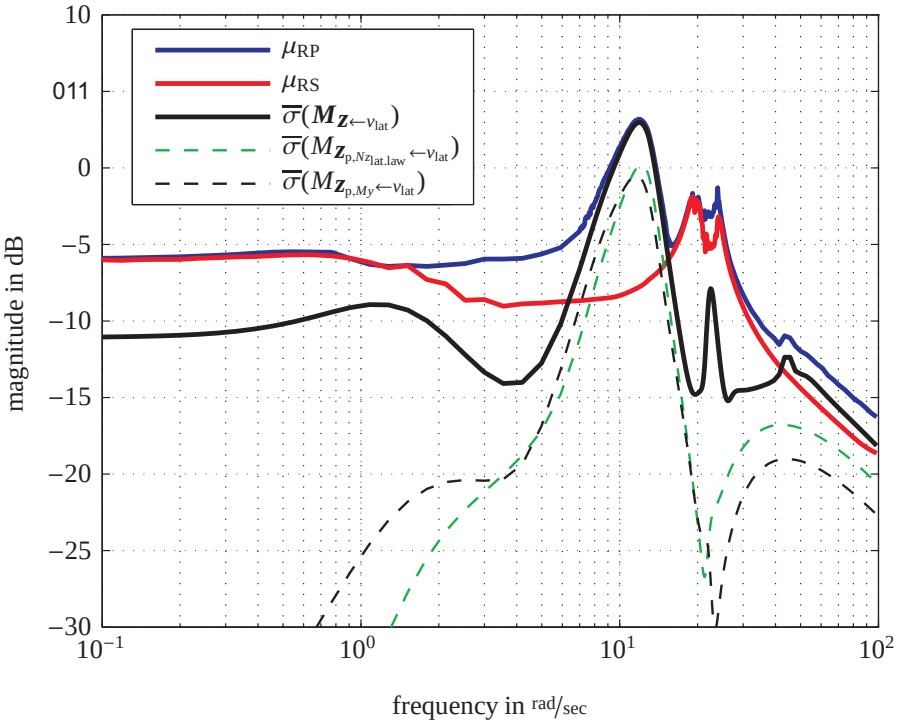


Figure 7: Nominal performance singular values and $\mu$ upper bounds for RP and RS

## 4. Validation, Performance, and Discussion

### 4.1 Validation of Control Performance and Robustness

The control law obtained in Sec. 3.3.3 is validated with all grid models (1)–(2). All closed-loop systems are stable. Fig. 8 shows the magnitude plots of the disturbance – performance paths: the first flexible mode can robustly be reduced to 2–3 dB below the level provided by the initial control law.

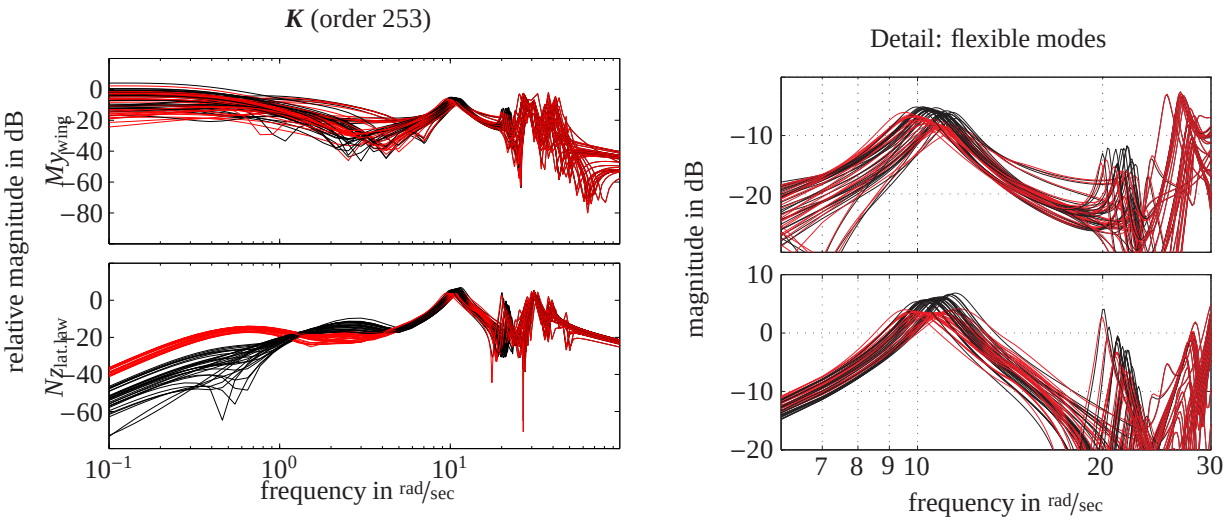


Figure 8: Bode magnitude plots of (von-Karman low-pass filtered) lateral wind $v_{\text{lat}}$ - wing cut moment $My_{\text{wing}}$ and modal acceleration signal $Nz_{\text{lat.law}}$ for all mass cases (black: aircraft model with initial control law only, red: closed loop with initial controller and robust controller, obtained by DGK-iteration with the reduced-accuracy design LFR)

### 4.2 Discussion

A highly detailed modeling process yields accurate system models for a parameter grid of relevant system parameters. For high parameterization accuracy, the obtained parameterized Linear Fractional Representation turns out to be prohibitively complex for current $\mu$ analysis and synthesis algorithms. Several ways to solve the design task have been attempted, including well-known problem regularization techniques ("complexification" of the uncertainty description) and simplification of the Linear Fractional Representation.

Ad-hoc uncertainty modeling yields simple LFRs and high control performance for the design plant, but it destabilizes some parameter-extremal validation plant cases in closed loop. No straightforward remedy is found without compromising control performance significantly.

Subsequently, a reduced-accuracy parameterized LFR is generated which leads to a successful, albeit computationally demanding design. The obtained control law can be reduced to order 30 without performance degradation and yields stable closed loops with all validation cases. Its performance is significantly lower than the nominal performance achieved through the ad-hoc approach, but in turn it provides an actually robust solution. Considering that significant damping is already introduced by the initial control law it is plausible that further improvement comes at high cost – both in terms of design complexity as well as numeric complexity of the control law.

As an outlook to possible future research, several other approaches could be attempted in such high-complexity designs. To meet the numeric challenges associated to $\mu$ bounds calculation, especially in the present case where a low number of parameters is repeated often, it seems reasonable to attempt numeric search methods to empirically find improved $\mu$ bounds. Also, $\mu$ computation algorithms without the need of fine frequency gridding could alleviate the encountered difficulties [5].

In conclusion, these findings underline the importance of efficient LFR modeling for DK-/DGK-iteration-based control design. The encountered challenges demonstrate the need for algorithms which allow to generate efficient LFRs whose parameterization accuracy is optimized for the envisaged control task, for example through frequency-weighted error minimization.

## 5. Conclusions

This paper presents first results for the robust feedback control design of lateral inner-loop control laws for a large BWB passenger aircraft pre-design model. Starting with an initial control law that already provides basic response shaping and flexible mode damping, the main design goal here is to further increase the damping of the flexible modes robustly despite strong parameter-dependent plant variation. The DGK-iteration synthesis procedure is utilized and several LFR formulations of the aircraft model parameter dependency are utilized. The highest-complexity attempt involving a high-accuracy parametric LFR cannot be handled computationally. A simple, manual ad-hoc uncertainty formulation leads to quick results with high nominal performance but fails to provide robustness in validation. Finally, a reduced-accuracy parametric LFR is utilized which leads to a computationally demanding design, but yields a control law that robustly stabilizes and attenuates the flexible dynamics above the level provided by the initial control law.

## Acknowledgements

This work was financially supported by the European Union Framework Programme 7 under the FP7 project number 213321 [1].

## References

[1] ACFA 2020 Consortium. Active control of flexible 2020 aircraft (ACFA 2020), EU FP7 project no. 213321. URL: http://www.acfa2020.eu, retrieved: Jan. 31st, 2011.

[2] G. Balas, R. Chiang, A. Packard, and M. Safonov. *MATLAB Robust Control Toolbox 3, User's Guide*. MathWorks, 2010.

[3] C. Benatzky. *Theoretical and experimental investigation of an active vibration damping concept for metro vehicles*. Dissertation, Vienna University of Technology, Vienna, 2006.

[4] V. R. Dehkordi and B. Boulet. Robust controller order reduction. In *Proc. American Control Conf.*, pages 3083–3088, USA, 2009.

[5] G. Ferreres and J.M. Biannic. A $\mu$ analysis technique without frequency gridding. In *American Control Conference, 1998. Proceedings of the 1998*, volume 4, pages 2294–2298. IEEE, 1998.

[6] W. Gawronski. *Advanced structural dynamics and active control of structures*. Springer, New York, 2004.

[7] D.W. Gu, P.H. Petkov, and M.M. Konstantinov. *Robust control design with MATLAB*, volume 1. Springer Verlag, 2005.

[8] M. Hanel. *Robust Integrated Flight and Aeroelastic Control System Design for a Large Transport Aircraft*. Number 866 in 8. VDI-Verlag, 2001.

[9] S. Hecker. *Generation of low order LFT Representations for Robust Control Applications*. PhD thesis, Technische Universität München, 2006.

[10] M. Jeanneau, J. Lamolie, G. Puyou, and N. Aversa. Awiator´s design of multi-objectives control laws. *IFAC*, 2005.

[11] A. Kron, J. de Lafontaine, and D. Alazard. Robust 2-DOF H-infinity controller for highly flexible aircraft: Design methodology and numerical results. *Canadian Aeronautics and Space Journal*, 49:19–29, 2003.

[12] J.-F. Magni. *Robust Modal Control with a Toolbox for Use with MATLAB*. Kluwer Academic, 2002.

[13] B. Mialon and M. Hepperle. Flying wing aerodynamics studies at ONERA and DLR. In *CEAS Katnet Conference on Key Aerodynamic Technologies*, Germany, 2005.

[14] MG Safonov and RY Chiang. Model reduction for robust control: A schur relative error method. *International Journal of Adaptive Control and Signal Processing*, 2(4):259–272, 1988.

[15] A. Schirrer, C. Westermayer, M. Hemedi, and M. Kozek. A comprehensive robust control design and optimization methodology for complex flexible-structure systems. In *Proc. of the 18th Mediterranean Conf. on Control and Automation*, Marrakech, Morocco, 2010.

[16] A. Schirrer, C. Westermayer, M. Hemedi, and M. Kozek. LQ-based design of the inner loop lateral control for a large flexible BWB-type aircraft. In *2010 IEEE Multi-Conf. on Systems and Control*, Yokohama, Japan, 2010.

[17] A. Schirrer, C. Westermayer, M. Hemedi, and M. Kozek. Multi-model convex design of a scheduled lateral feedforward control law for a large flexible BWB aircraft. In *Proc. 18th IFAC World Congress (submitted)*, 2010.

[18] A. Schirrer, C. Westermayer, M. Hemedi, and M. Kozek. Robust convex lateral feedback control synthesis for a large flexible BWB aircraft. In *Proc. 18th IFAC World Congress (submitted)*, 2010.

[19] A. Schirrer, C. Westermayer, M. Hemedi, and M. Kozek. Robust $\mathcal{H}_\infty$ control design parameter optimization via genetic algorithm for lateral control of a BWB type aircraft. In *IFAC Workshop on Intell. Control Systems*, Sinaia, Romania, 2010.

[20] S. Skogestad and I. Postlethwaite. *Multivariable Feedback Control Analysis and Design*. John Wiley & Sons, 1996.

[21] F. Stroscher, Ö. Petersson, and M. Leitner. Aircraft structural optimization subject to flight loads - application to a wide body commercial aircraft configuration. In *EASN Intl. Workshop on Aerostructures*, October 2010.

[22] C. Westermayer, A. Schirrer, M. Hemedi, and M. Kozek. Linear parameter-varying control of a large blended wing body flexible aircraft. In *18th IFAC Symposium on Automatic Control in Aerospace*, Nara, Japan, 2010.

[23] C. Westermayer, A. Schirrer, M. Hemedi, M. Kozek, and A. Wildschek. Robust $\mathcal{H}_\infty$ flight and load control of a flexible aircraft using a 2DOF multi-objective design. In *Proceedings of 2009 CACS International Automatic Control Conference*, 2009.

[24] A. Wildschek, R. Maier, M. Hromcik, T. Hanis, A. Schirrer, M. Kozek, Ch. Westermayer, and M. Hemedi. Hybrid controller for gust load alleviation and ride comfort improvement using direct lift control flaps. *Proc. of the 3rd EuCASS*, 2009.

[25] K. Zhou, J. C. Doyle, and K. Glover. *Robust and optimal control*. Prentice Hall, 1996.